COBEM 2023 27TH INTERNATIONAL CONGRESS OF MECHANICAL ENGINEERING

ABCM Brazilian Society of Mechanical Sciences and Engineering
27th ABCM International Congress of Mechanical Engineering
December 04-08, 2023, Florianópolis-SC, Brazil

COB-2023-1604
NUMERICAL EVALUATION OF ITERATIVE METHODS FOR CALCULATING FREQUENCY RESPONSE FUNCTIONS OF DYNAMIC STRUCTURES COMPOSED OF VISCOELASTIC MATERIALS

Luiz Otávio Rigobello Muraro
Sandmara Lanhi
Jucélio Tomás Pereira
Simone de Fátima Tomazzoni Gonçalves
Federal University of Paraná, Polytechnic Center, 100 Cel. Francisco H. dos Santos, Curitiba PR 81530-000
luizotaviorigobello@gmail.com; sandmara_lanhi@hotmail.com; jucelio.tomas@ufpr.br; simone.tg@ufpr.br

Abstract. *In the passive vibration control, the use of viscoelastic materials (VEM) is well-known. This is mainly due to their high capacity for dissipating vibratory energy. Therefore, understanding the dynamic behavior of structures composed of VEM is fundamental. To do so, it is necessary to obtain the frequency response functions (FRFs) of the structure. However, dynamic analyses of this type of structure involve frequency-dependent parameters and this makes the formulations computationally expensive when used in systems with many degrees of freedom. In this context, the objective of this study is to numerically evaluate different iterative methods, based on Krylov subspace, for the solution of complex linear systems for calculating FRFs of dynamic structures composed of viscoelastic materials and with a high number of degrees of freedom. For this purpose, a bar composed of VEM and metallic material will be discretized via finite element method (FEM) into one-dimensional elements. With this structure, the FRFs will be evaluated numerically using the direct method (reference method) and two iterative methods (Minimun Residual and Symmetric LQ) and then compared with a modal truncation method. The processing times and a graphical analysis of the convergence of the methods were presented.*

Keywords: *Finite Element Method, Passive Vibration Control, Receptance, Krylov Subspace.*

1. INTRODUCTION

Vibration can be defined as the repetitive motion observed concerning a reference position (Rao, 2011). Nonetheless, this oscillatory movement often leads to significant issues in various systems and structures. Notably, vibrations can cause acoustic discomfort, reduce the overall performance of the structure, induce wear and tear in bearings, and subsequently, hamper competitiveness in the market. In extreme and not uncommon scenarios, fatigue from these vibrations can even compromise the system's lifespan, potentially leading to catastrophic fractures. Therefore, implementing some form of control mechanism becomes indispensable to effectively mitigate these challenges.

Recent studies have addressed vibration reduction in transmission towers, such as the one conducted by Roy and Kundu (2021), as well as the analysis of advanced vibration reduction techniques in wind turbines, exemplified by Xie et al. (2020). In addition to these studies, there are several other examples of vibration control documented in the literature, including research carried out by Kandasamy et al. (2016), Ji et al. (2021), and Gao et al. (2022).

Among the various approaches to vibration control, passive methods have gained widespread usage due to their self-sufficiency, not relying on external energy sources, and their ease of application and maintenance. This method typically involves incorporating devices and/or materials that dissipate vibrational energy into the system requiring control. For instance, the utilization of viscoelastic materials, which demonstrate characteristics of absorbing vibrational energy and storing elastic potential energy. As stated by Floody et al. (2007), these properties arise from the coexistence of both viscous and elastic behaviors within the material. In this context, comprehending the dynamic behavior of structures comprised of viscoelastic materials becomes paramount.

The dynamic behavior of a system can be derived through Frequency Response Functions (FRFs). FRFs are obtained in the frequency domain and offer valuable insights into the system's dynamic characteristics, considering a specific degree of freedom for excitation and response. By utilizing FRFs, one can determine the system's natural frequencies and examine the amplitudes of displacement, velocity, and acceleration at each excitation frequency. However, acquiring FRFs necessitates solving the system's equation of motion and obtaining the mass, stiffness, and damping matrices of the system (Rao, 2011).

One well-known approach to obtain the mass and stiffness matrices required for this calculation is by using the Finite Element Method (FEM). When applied to structures with many degrees of freedom n, the FEM generates very high-order matrices. Additionally, in the case of VEMs, the stiffness matrix is frequency-dependent, leading to the

solution of a nonlinear eigenproblem. In the literature, various methods have been employed to tackle this type of problem, including the direct solution method, modal superposition method, and eigenvalue-based methods such as the Lanczos method (LANCZOS, 1950) and the subspace iteration method (BATHE, 1996).

The direct solution methods rely on the exact resolution of a complex linear system for each discrete frequency value within the interval of interest. Nevertheless, this approach can result in a significantly high computational cost, especially for systems with a large number of degrees of freedom. To mitigate processing time, Floody et al. (2007) developed a method that involves truncating the first $\hat{n}$ columns of the modal matrix, considering a fixed frequency corresponding to the first $\hat{n}$ vibration modes. Subsequently, for each frequency within the interval of interest, an eigenvalue/eigenvector problem of order $\hat{n} \times \hat{n}$ is solved. The results showed a close approximation when compared with experimental values. Bortolloto et al. (2013) replaced the $\hat{n} \times \hat{n}$ eigenproblem with a direct solution of a linear system of equations of the same order. Furthermore, the authors experimented with various fixed frequencies for the first eigenvalue and the subsequent number of modes $\hat{n}$ used in the method. Kanke et al. (2022) applied this methodology to passive vibration control in plates through the optimization of restricted layer topologies.

There are other recent lines of study aiming to replicate the dynamic behavior of structures composed of VEM and successfully exhibit this frequency dependency. Some of these studies were conducted by Ingman and Suzdalnilsky (2001), Martin (2016), Łasecka-Plura and Lewandowski (2021), and Jiao et al. (2022). However, there are still few studies that compare computational cost and convergence using iterative methods applied to the utilization of MEV. This work aims to propose a new iterative methodology employing Krylov subspace methods (MINRES and SYMMLQ) (Paige and Saunders, 1975) at its intermediate stage. The objective is to provide an alternative to existing methods, numerically evaluate the processing time and convergence, and compare it with the method proposed by Bortolloto et al. (2013) and a direct solution method used as a reference.

2. VISCOELASTIC MATERIALS

Viscoelastic materials (VEM) are used in various applications, including the naval, automotive, aerospace, and structural sectors. This is attributed to their high capacity to dissipate vibrational energy and their ease of application. Nonetheless, the mechanical behavior of these materials is strongly dependent on frequency and temperature (Mainardi, 2022). The relationship between these two variables is given by the shift factor α_T, which is described by the equation,

$$\Omega_r = \alpha_T \Omega, \tag{1}$$

where Ω represents the frequency, and Ω_r is known as the reduced frequency. This factor enables the approximation of the mechanical property curve of the VEM without the need for numerous experimental tests at that specific temperature, thereby relating it to a reduced frequency curve. In the literature, various shift factors can be found, but the most used is the model developed by Williams-Landel-Ferry (WLF) (Tcharkhtchi et al., 2015), which satisfactorily reproduces this behavior. The shift factor proposed by Williams-Landel-Ferry is given by the equation,

$$log\ \alpha_T = -\frac{\theta_1 (T - T_0)}{\theta_2 + (T - T_0)}, \tag{2}$$

in which θ_1 and θ_2 are material parameters obtained experimentally, T represents the working temperature, and T_0 is the reference temperature. Using Eq. (2), it is possible to obtain other viscoelastic properties, such as the complex modulus of elasticity and shear modulus, for different temperatures and frequencies. In this work, the complex modulus of elasticity, E_c, is obtained using the four-parameter fractional Zener model (Findley and Davis, 2013), (Mainardi, 2022), given by

$$E_c = \frac{(E_0 + E_\infty\ a(i\Omega_r)^\beta)}{(1 + a(i\Omega_r)^\beta)}, \tag{3}$$

3. FREQUENCY RESPONSE FUNCTION OF A DYNAMIC SYSTEM COMPOSED OF METAL AND VISCOELASTIC MATERIAL

To solve a vibration problem of a specific system or structure, it is necessary to resolve the equation of motion. In this case, considering the equation of motion in the frequency domain, in matrix form, for a harmonic system composed of metal and viscoelastic material,

$$[[K(\Omega)] + i\Omega[C] - \Omega^2[M]]\{X(\Omega)\} = \{\mathrm{F}(\Omega)\}, \tag{4}$$

where $[M]$, $[C]$, and $[K(\Omega)]$ are, respectively, the global mass, damping, and stiffness matrices of the system. $\{X(\Omega)\}$ and $\{\mathrm{F}(\Omega)\}$ represent the generalized displacement response and generalized excitation force vectors of the system. n Eq. (4), it is evident that the stiffness matrix is frequency-dependent. This dependence is related exclusively to the viscoelastic portion of the material. The global stiffness matrix of the system is the sum of the viscoelastic portion (represented by the submatrix $[K_v(\Omega)]$), and the purely elastic portion corresponding to the metallic material (represented by the submatrix $[K_m]$). Thus, the global stiffness matrix of the system can be expressed as

$$[K(\Omega)] = [K_m] + [K_v(\Omega)]. \tag{5}$$

The portion corresponding to the metallic material, $[K_m]$, consists of real and constant values. On the other hand, the part associated with the stiffness matrix of the VEM, $[K_v(\Omega)]$, comprises complex values that are dependent on frequency and temperature.

To obtain the Frequency Response Function (FRF) of the harmonic system, it is necessary to directly solve Eq. (4) for each discrete frequency value. The FRF that relates the displacement response to the excitation force is defined by the equation,

$$H_{ks} = \frac{\{X_k(\Omega)\}}{\{F_s(\Omega)\}} = \left([K(\Omega)] + i\Omega[C] - \Omega^2\,[M]\right)^{-1}_{ks}, \tag{6}$$

and is known as receptance, H_{ks}. The receptance H_{ks} represents the generalized displacement response of the structure at the degree of freedom k, resulting from a point excitation applied at degree of freedom s, for each excitation frequency value Ω. Notwithstanding, for a system with a large number of degrees of freedom and frequency discretization, solving high-order linear systems becomes computationally expensive. The method presented by Floody et al. (2007), modified by Bortolloto et al. (2013), aims to provide a viable approximation for obtaining the FRFs of systems composed of metal and VEM. This method will be further discussed in the next section.

3.1 Modal Matrix Truncation Methodology

This method has the general characteristic of reducing the system's order of equations, then minimizing the number of operations and, consequently, reducing the processing time. The method begins with the selection of a reference frequency Ω_0, which should belong to the frequency range under analysis. According to Floody et al. (2007), this variable significantly influences the results, especially when considering temperature variations. In this study, a constant working temperature of the VEM is assumed.

Once the reference frequency is defined, the stiffness matrix of the viscoelastic material is calculated using Eq. (5), where the term corresponding to the viscoelastic component is given by,

$$[K_v(\Omega_0)] = E(\Omega_0)[K_v'], \tag{7}$$

where $[K_v']$ is the stiffness matrix obtained considering a unitary elasticity modulus (1 N/m²). It is observed that in this equation, the only frequency-dependent term is the complex elasticity modulus $E(\Omega_0)$, which is obtained through Eq. (3). After this step, an eigenvalue problem, associated with the mass and stiffness matrices of the global system is solved for that reference frequency $K(\Omega_0)$, according to the equation,

$$\lambda_i[M]\{\phi_i\} = [K(\Omega_0)]\{\phi_i\}, \tag{8}$$

involving the index i varying from 1 to the total number of degrees of freedom of the system, n. The i-th eigenvalue is represented by λ_i, and $\{\phi_i\}$ is the corresponding i-th eigenvector. The modal matrix $[\Phi_0] = [\phi_1, \phi_2, \phi_3, \dots, \phi_n]$, can be defined, and its columns are the eigenvectors obtained in Eq. (8).

This method assumes that only the first few vibration modes significantly contribute to the receptance response. Thus, the modal matrix, Φ_0, evaluated at the reference frequency, can be truncated to the first nˆ vibration modes (columns), where $\hat{n} \ll n$. This truncated modal matrix is denoted as $\widehat{\Phi}_0$ and has a size of $n \times \hat{n}$, with n being the total number of degrees of freedom of the structure. By arranging the eigenvalues in ascending order and performing the corresponding reordering of the modal matrix and orthogonalizing it with respect to the mass matrix, the following properties can be observed,

$$\left[\widehat{\Phi}_0\right]^T[M]\left[\widehat{\Phi}_0\right] = [I]_{\hat{n}\times\hat{n}}, \tag{9}$$

and,

$$\left[\widehat{\Phi}_0\right]^T[K(\Omega_0)]\left[\widehat{\Phi}_0\right] = [\Lambda]_{\hat{n}\times\hat{n}}, \tag{10}$$

in which, $\left[\widehat{\Phi}_0\right]^T$ represents the transposed matrix of the truncated modal matrix. $[I]_{\hat{n}\times\hat{n}}$ and $[\Lambda]_{\hat{n}\times\hat{n}}$ correspond, respectively, to the identity matrix and the spectral matrix of dimension $\hat{n}\times\hat{n}$.

In this method, the stiffness matrix is updated for each discrete frequency value through an incremental process. This method applies an increment in the material property value, $\Delta E(\Omega;\Omega_0)$, based on the elasticity modulus from the reference frequency and isolates this term using the equation,

$$\Delta E(\Omega;\Omega_0) = E(\Omega) - E(\Omega_0). \tag{11}$$

Thus, the stiffness matrix can be found for each discrete frequency value using Eq. (5) and Eq. (7), as follows,

$$[K(\Omega)] = [K_m] + E(\Omega)[K_v'] = [K_m] + E(\Omega_0)[K_v'] + \Delta E(\Omega;\Omega_0)[K_v'] = [K(\Omega_0)] + \Delta E(\Omega;\Omega_0)[K_v']. \tag{12}$$

Assuming a change of coordinates from the physical system to the truncated modal space in the form of,

$$\{X(\Omega)\} = \left[\widehat{\Phi}_0\right]\{P(\Omega)\}, \tag{13}$$

and pre-multiplying Eq. (4) by $\left[\widehat{\Phi}_0\right]^T$, results in

$$\left[-\Omega^2\left[\widehat{\Phi}_0\right]^T[M]\left[\widehat{\Phi}_0\right] + i\Omega\left[\widehat{\Phi}_0\right]^T[C]\left[\widehat{\Phi}_0\right] + \left[\widehat{\Phi}_0\right]^T[K(\Omega)]\left[\widehat{\Phi}_0\right]\right]\{P(\Omega)\} = \left[\widehat{\Phi}_0\right]^T\{F(\Omega)\}. \tag{14}$$

Subsequently, Eq. (12), obtained earlier, is used to replace the stiffness matrix as

$$\left[\widehat{\Phi}_0\right]^T[K(\Omega)]\left[\widehat{\Phi}_0\right] = \left[\widehat{\Phi}_0\right]^T[K(\Omega_0)]\left[\widehat{\Phi}_0\right] + \Delta E(\Omega;\Omega_0)\left[\widehat{\Phi}_0\right]^T[K_v']\left[\widehat{\Phi}_0\right]. \tag{15}$$

By applying the properties presented in Eq. (9) and Eq. (10), a new system of equations is then solved, given by

$$[-\Omega^2[I]_{\hat{n}\times\hat{n}} + i\Omega[\tau]_{\hat{n}\times\hat{n}} + [\Lambda]_{\hat{n}\times\hat{n}} + \Delta E(\Omega;\Omega_0)[\Lambda_v']_{\hat{n}\times\hat{n}}]\{P(\Omega)\} = \left[\widehat{\Phi}_0\right]^T\{F(\Omega)\}, \tag{16}$$

where $[\Lambda_v']_{\hat{n}\times\hat{n}} = \left[\widehat{\Phi}_0\right]^T[K_v']\left[\widehat{\Phi}_0\right]$, $[\tau]_{\hat{n}\times\hat{n}} = \left[\widehat{\Phi}_0\right]^T[C]\left[\widehat{\Phi}_0\right]$, and $[\Lambda]_{\hat{n}\times\hat{n}}$ are diagonal and constant matrices. It can be observed in Eq. (16) that the only variable dependent on frequency is $\Delta E(\Omega;\Omega_0)$, and the order of this new system of equations is $\hat{n}\times\hat{n}$, significantly smaller than the original system in Eq. (4). Furthermore, the matrices $[I]_{\hat{n}\times\hat{n}}$, $[\tau]_{\hat{n}\times\hat{n}}$, and $[\Lambda]_{\hat{n}\times\hat{n}}$ are diagonal. This results in a smaller number of arithmetic operations, thus saving processing time.

Finally, returning to the geometric coordinate system, the displacement response for a structure composed of metallic material and VEM can be obtained for a given frequency, expressed as

$$\{X(\Omega)\} = \left[\widehat{\Phi}_0\right][-\Omega^2[I]_{\hat{n}\times\hat{n}} + i\Omega[\tau]_{\hat{n}\times\hat{n}} + [\Lambda]_{\hat{n}\times\hat{n}} + \Delta E(\Omega;\Omega_0)[\Lambda_v]_{\hat{n}\times\hat{n}}]^{-1}\left[\widehat{\Phi}_0\right]^T\{F(\Omega)\}, \tag{17}$$

in which $[\ \ ]^{-1}$ denotes the matrix inverse, this equation merely represents the calculation, though. In practice, it is not computed directly, but instead, it involves solving a linear system of equations of order $\hat{n}\times\hat{n}$ from Eq. (14) and then undergoing a change of coordinates expressed by Eq. (13).

3.2 Iterative metodology proposed

Structures employing passive control with VEM are illustrative examples of systems featuring frequency-dependent parameters. This frequency dependency introduces nonlinearity into the set of equations, which can be addressed through frequency discretization, treating it as a linear system for each discrete point. Therefore, in Eq. (4), we encounter a system of linear equations, whereby the term $[[K(\Omega)] + i\Omega[C] - \Omega^2\,[M]]$ denotes the coefficient matrix of this system, characterized by its symmetry and inclusion of complex terms.

This system can be solved using direct methods, such as LU decomposition, which are widely employed in commercial software. Direct methods, including LU decomposition, are known for their robustness and efficiency, but for this particular type of structure, they require a substantial number of arithmetic operations for each discrete frequency value within the specified interval. Consequently, this process becomes computationally expensive.

As an alternative to direct methods, iterative approaches can be employed. In these methods, convergence to an approximate solution is achieved by iteratively updating a sequence of vectors derived from an initial vector X_0. In this study, two iterative methods will be tested to solve the system in Eq. (4). To achieve this, the initial vector is set to be

equal to the approximate solution vector obtained for a previous frequency, along with the addition of the vector difference between the two previous response vectors. This is represented by the equation,

$$\{X_0(\Omega_j)\} = \{X(\Omega_{i-1})\} + \{\Delta X\}, \tag{18}$$

in which,

$$\{\Delta X\} = \{X(\Omega_{i-1})\} - \{X(\Omega_{i-2})\}, \tag{19}$$

where the index j ranges from 3 to N_i (number of frequency discretization points). For i=1, the initial vector is set to be a null vector, and for i=2, $\{X_0(\Omega_2)\} = \{X(\Omega_1)\}$.

The selected iterative methods for testing in this study are Minimum Residual (MINRES) and Symmetric LQ (SYMMLQ) (Paige and Saunders, 1975). These methods are variations of the Lanczos method designed to handle cases involving indefinite symmetric matrices and are widely employed in commercial software. To accelerate the convergence of the method, a preconditioning matrix is utilized (Saad, 2003) and applied across all frequencies. Hence, a matrix is chosen with coefficients that remain independent of this variable. An approach known as Incomplete LU, based on the damping matrix $[C]$ of the system, has been chosen. In this study, this matrix is obtained through the formulation of proportional damping (Petyt, 2010) for the primary system, representing only the metallic portion of the structure.

To enhance clarity of the proposed methodology, a pseudo-code is provided below:

1. *Define* $[M_p], [M_t], [K_m], [K_v'], \{F\}$;
2. *Calculate* $[C]$;
3. *Calculate preconditioned matriz by incomplete LU factorization.*
4. *For* $j = 1, \dots, N_i$, *Do:*
5. *Compute* $E_c(\Omega_j)$ – *Eq. (3);*
6. *Compute* $[K(\Omega_j)]$ – *Eq. (5);*
7. *Solve by MINRES or SYMMLQ* $\{X(\Omega_j)\}$ – *Eq. (4);*
8. *Calculate* $\{\Delta X\}$ – *Eq. (19);*
9. *Calculate* $\{X_0(\Omega_j)\}$ – *Eq. (18);*
10. *Save* $H_{ks}(\Omega_j)$ = *X(k);*
11. *EndDo.*

Here, M_p and M represent the mass matrices of the primary system and the total system, respectively, while N_i denotes the number of frequency discretization points. The next section will present the methodology employed in this study.

4. METHODOLOGY

In this numerical study, all calculations were performed using MATLAB-r2018 software. The analysis focused on vibrations in a one-dimensional (1-D) bar composed of metallic material and VEM. The VEM was positioned between two identical layers of metallic material. Figure 1 illustrates the generalized structure and its dimensions

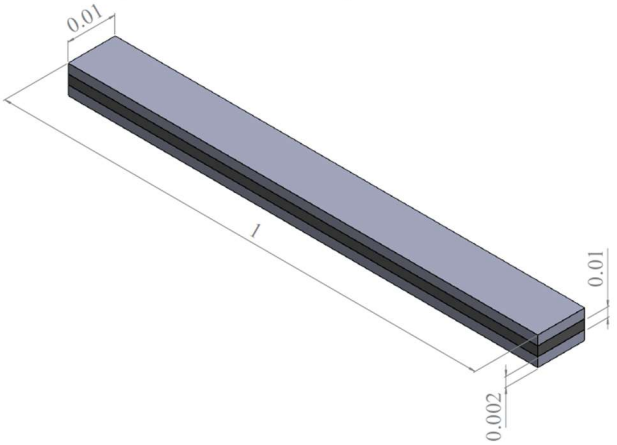

Figure 1. Dimensions in meters of the Bar of Metal and VEM

The metallic material is ASTM A36 steel, with a modulus of elasticity equal to 200 GPa and a specific mass of 7860 Kg/m³. The selected viscoelastic material is EAR C-1002, and its mechanical properties, as presented in Silva et al. (2019) and described in Table 1, were employed in the analysis.

Table 1. Parameters of the viscoelastic material - EAR C-1002

Specific Mass ρ (kg/m³)	**E_0 (MPa)**	**E_∞ (GPa)**	**a -**	**β -**	**θ_1 -**	**θ_2 (K)**
1289	1.927	2.706	2.089E-03	0.538	34.67	607.07

The shift factor, α_T, was computed using a reference temperature of 285.15 K and a working temperature of 303.15 K. The elements were discretized and arranged in ascending order, as illustrated in Figure 2.

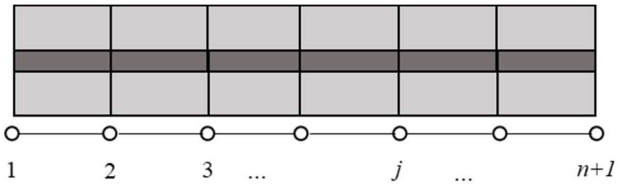

Figure 2. Schematic discretization of the Finite Element Method in bar element

The Dirichlet boundary condition corresponds to the clamped end at node 1 on the left side of the bar. On the other hand, the Neumann boundary condition is characterized by the application of an axial tensile force $\{F(\Omega)\}$ at node $n+1$, on the right end of the bar. Three different discretization sizes, with n elements and $n+1$ nodes, were subjected to testing: 16384 (2^14), 65536 (2^16), and 262144 (2^18) nodes. Employing this discretization approach, the Finite Element Method (FEM) was utilized to calculate the symmetric and tridiagonal matrices $[M_p]$, $[M_t]$, $[K_m]$, and $[K_v']$, which play a significant role in the problem. For the frequency range, the selected interval was from 500 to 7000 Hz, and two discretization schemes were considered: 1 - 1 Hz (6501 points) and 0.2 – 0.2 Hz (32501 points).

For the direct method, the MATLAB – r2018 command \ was used, which employs LU decomposition for this type of equation. The matrix modal truncation methodology (Bortolloto et al., 2013) was implemented using MATLAB – r2018, considering a reference frequency of 3750 Hz and truncating to the first 30 modes. As for the iterative methodology, the MINRES and SYMMLQ commands of MATLAB – r2018 were utilized, corresponding to the minimum residual and symmetric LQ methods, respectively.

5. DISCUSSION AND RESULTS

The matrix receptance element being evaluated corresponds to the node *n+1*, for both excitation and response. The CPU time for each method exclusively represents the time required to solve the N_i (number of frequency discretization points) systems of linear equations. Additionally, the relative time for each method was calculated, which is obtained by,

$$Relative\ time\ (Method) = \frac{CPU\ time\ (Method)}{CPU\ time\ (LU)}. \tag{20}$$

In this context, the method utilizing LU decomposition was used as the reference time. Table 2 presents the CPU time and relative time for N_i equal to 6501 points in frequency, meaning that the frequency varies from 1 Hz to the next. It can be observed that only Bortolloto et al.'s method (2013) has a CPU time lower than the LU decomposition for all system order sizes. As a result, it yields a relative time less than one. Moreover, the relative time for this method remains relatively constant regardless of the system's size, as it does not exhibit significant variations despite the increase in the system's order, n.

Table 2 clearly shows that the two iterative methods were not effective for N_i = 6501 across all mesh sizes. In contrast, Table 3 presents the CPU time and relative time for a discretization with an incremental frequency of 0.2 Hz (N_i=32501). Once again, Bortolloto et al.'s method (2013) exhibited the lowest CPU time and the best relative time compared to those in Table 2.

Regarding the iterative methods, a notable observation in Table 3 is that for n = 262144, the relative time is less than 1, indicating their superiority over the reference method in terms of speed. This outcome could be attributed to the increased number of points in the incremental process, allowing the iterative process to start closer to the final solution for each frequency, resulting in faster convergence for N_i = 6501. Additionally, the tolerance chosen for the iterative

method significantly affected the CPU time, with a lower tolerance resulting in higher computational cost but providing a final solution closer to the reference.

Table 2. CPU time and Relative time 1 - 1 Hz (N_i=6501)

Method of solution	Tolerance	Result	Order of the system		
			16384	65536	262144
Direct – LU decomposition	-	CPU [s]	14.3156	58.2906	239.8591
MINRES	E-04	CPU [s]	19.4662	61.1219	188.9037
		Relative Time	1.3598	1.0486	0.7876
MINRES	E-05	CPU [s]	23.4762	81.7944	249.6520
		Relative Time	1.6399	1.4032	1.0408
MINRES	E-06	CPU [s]	31.6436	108.0238	326.9746
		Relative Time	2.2104	1.8532	1.3632
SYMMLQ	E-04	CPU [s]	21.7049	72.8752	252.4416
		Relative Time	1.5162	1.2502	1.0525
SYMMLQ	E-05	CPU [s]	25.8546	87.0353	270.2612
		Relative Time	1.8060	1.4931	1.1267
SYMMLQ	E-06	CPU [s]	34.2878	111.0568	351.9529
		Relative Time	2.3951	1.9052	1.4673
Bortolloto et al., (2013)	-	CPU [s]	4.0101	16.8237	69.8099
		Relative Time	0.2801	0.2886	0.2910

Table 3. CPU and relative time 0.2 - 0.2 Hz (N_i=32501)

Method of solution	Tolerance	Result	Order of the system		
			16384	65536	262144
Direct – LU decomposition	-	CPU [s]	70.6761	291.7863	1195.10
MINRES	E-04	CPU [s]	87.5340	290.5882	858.3975
		Relative Time	1.2385	0.9959	0.7183
MINRES	E-05	CPU [s]	91.2626	307.3477	928.6896
		Relative Time	1.2913	1.0533	0.7771
MINRES	E-06	CPU [s]	102.2242	335.3513	1115.70
		Relative Time	1.4464	1.1493	0.9336
SYMMLQ	E-04	CPU [s]	96.2100	320.3621	912.0847
		Relative Time	1.3613	1.0979	0.7632
SYMMLQ	E-05	CPU [s]	107.8995	357.9434	1004.8000
		Relative Time	1.5267	1.2267	0.8408
SYMMLQ	E-06	CPU [s]	120.9945	385.2406	1197.1000
		Relative Time	1.7120	1.3203	1.0017
Bortolloto et al., (2013)	-	CPU [s]	17.3979	72.9832	311.1768
		Relative Time	0.2462	0.2501	0.2604

Tables 4 and 5 were generated by evaluating the maximum error with respect to the reference solution. This residual was calculated as the maximum difference between the receptances, using the following expression:

$$Maximum\ Error\ (Method) = Max\ (\ Absolute\{H(method)\} - \{H(\ LU\ decomposition)\}). \quad (21)$$

Table 4. Maximum error 1 - 1 Hz (N_i=6501)

Method of solution	Tolerance	Order of the system		
		16384	65536	262144
MINRES	E-04	3.1908E-08	7.3753E-08	1.9475E-07
MINRES	E-05	1.0662E-09	2.2903E-09	7.3314E-09
MINRES	E-06	3.3898E-11	8.2845E-11	3.1961E-10
SYMMLQ	E-04	2.1954E-08	5.9441E-08	1.3308E-07
SYMMLQ	E-05	6.7860E-10	3.1246E-09	7.7204E-05
SYMMLQ	E-06	3.4715E-11	8.6278E-11	3.0010E-10
Bortolloto et al., (2013)	-	2.6228E-06	2.2668E-06	2.6231E-06

Upon examining Table 4 and Table 5, it becomes evident that the Bortolloto et al. (2013) method exhibited higher absolute errors compared to all other methods. On the other hand, for the iterative approaches, reducing the tolerance

resulted in smaller errors. Furthermore, there was no substantial variation in the error with an increase in the system's order.

Table 5. maximum error 0.2 - 0.2 Hz (N_i=32501)

Method of solution	Tolerance	Order of the system		
		16384	65536	262144
MINRES	E-04	1.5443E-07	2.6715E-07	7.1879E-07
MINRES	E-05	4.2552E-09	1.5396E-08	2.6343E-08
MINRES	E-06	1.6008E-10	4.3726E-10	2.8557E-10
SYMMLQ	E-04	1.0856E-07	4.0654E-07	7.6068E-07
SYMMLQ	E-05	4.7967E-09	1.2673E-08	1.4423E-08
SYMMLQ	E-06	1.5695E-10	4.3325E-10	3.9763E-10
Bortolloto et al., (2013)	-	2.6228E-06	2.6228E-06	2.6231E-06

In Figure 3 (left), the receptance is shown for the Direct Method, Bortolloto et al. (2013) Method, MINRES, and SYMMLQ, consideringN_i = 32501 and n = 262144. The iterative methods were employed with a tolerance of E-05. Additionally, Figure 3 (right) provides a close-up view of the first peak in the receptance, showcasing how the iterative methods closely approximate the reference solution with high precision.

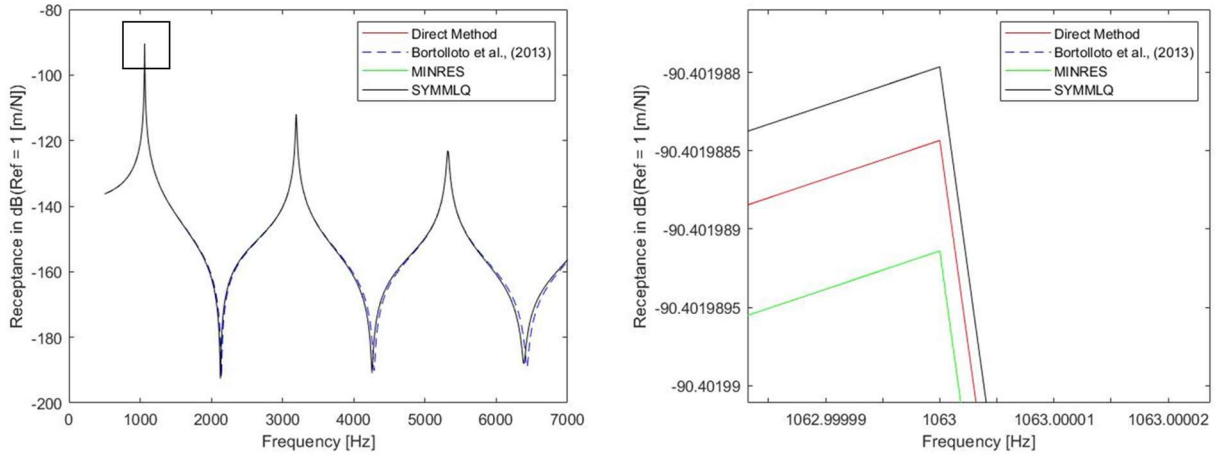

Figure 3. Receptance of the system with N_i = 32501, n = 262144 in all frequency interval (left)/ region in the black square (right).

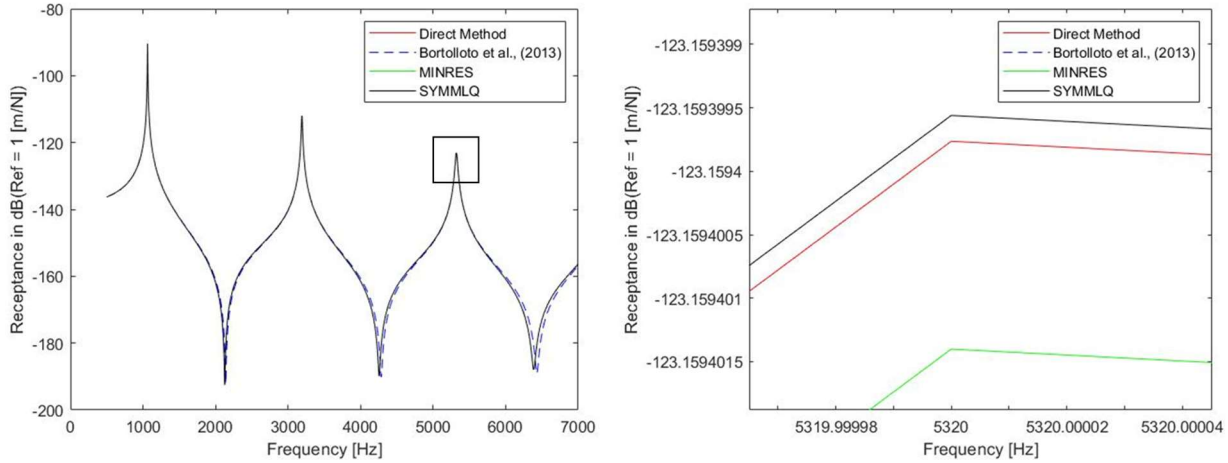

Figure 4. Receptance of the system with N_i = 6501, n = 65536 in all frequency interval (left)/ region in the black square (right).

Moreover, it is noticeable that the curves remain in close proximity to each other. However, as we approach the peak regions, only the iterative methods closely match the direct method with a precision of E-6. This indicates that the Method of Bortolloto et al. (2013) performs inadequately in these specific areas (E-1). We observe the same trend in

Figure 4, where the condition for N_i= 6501 and n = 65535 highlights the third peak region. Additionally, another notable observation from Figure 3 and Figure 4 is that the curve of the Method of Bortolloto et al. (2013) is slightly shifted to the right in the anti-resonance regions, leading to some distortion in the approximation. Based on the comprehensive analysis of the tables and graphs, we can confidently assert that the Modified Bortolloto et al. (2013) method offers the best CPU time in all conditions while exhibiting the worst curve approximation.

6. CONCLUSION

This study presented a methodology that tested two iterative methods (MINRES and SYMMLQ), in an incremental frequency process using an initial vector close to the convergent solution. These iterative methods were compared with the modal truncation method proposed by Bortolloto et al. (2013). However, they did not demonstrate effectiveness in terms of time when compared to the reference and the modal truncation methodology. It was observed that the relative times of the iterative methods were less than one for N_i = 32501 and n = 262144, indicating potential effectiveness for systems of larger orders. In terms of convergence, the iterative methods showed more favorable results compared to the method of Bortolloto et al. (2013), approaching the final solution more closely.

Although the CPU time did not meet the desired outcome for the iterative methods, future studies could explore potential modifications, such as using alternative preconditioning matrices or applying multigrid methods to solve the incremental process. Furthermore, there is ongoing research on the modified method proposed by Bortolloto et al. (2013), aiming to improve its convergence and reduce errors by considering a different approach to selecting the reference frequency.

7. ACKNOWLEDGEMENTS

The authors thank the Post-Graduated Program in Mechanical Engineering (PG-Mec) from Federal University of Paraná (UFPR), Brazil. Luiz Otávio Rigobello Muraro would like to thank the Coordenação de Aperfeiçoamento de Pessoal de Nível Superior (CAPES) for their financial support. Furthermore, Sandmara Lanhi would like to to acknowledge the Programa de Recursos Humanos da Agência Nacional de Petróleo, Gás Natural e Biocombustíveis (PRH-ANP).

8. REFERENCES

Bathe, K.-J., 1996. *Finite Element Procedures. Englewood Cliffs*. N.J: Prentice Hall, New Jersey.

Bortolotto, J.C., Lopes, E.M. O. and Bavastri, C.A., 2013, *Identificação e controle de vibrações de estruturas metálicas parcialmente compostas com lâminas viscoelásticas restringidas* (in Portuguese). In *Proceedings of The XXXIV Iberian Latin-American Congress on Computational Methods in Engineering*. *ABMEC, Pirenópolis, GO, Brazil, November 10-13, 2013*.

Findley, W.N. and Davis, F.A., 2013. *Creep and relaxation of nonlinear viscoelastic materials*. Dover publications, New York.

Floody, S.E., Arenas, J.P., and De Espindola, J.J., 2007. Modelling metal-elastomer composite structures using a finite element-method approach. Strojniski Vestnik, Vol. 53, pp. 66–77.

Gao, H., Hu, J., qi, Y. and Sun, C., 2022, Adaptive vibration control of a flexible structure based on hybrid learning controlled active mass damping, Journal of the Franklin Institute, Vol. 359, pp. 5935–5959.

Ingman, D., and Suzdalnitsky, J., 2001, Iteration method for equation of viscoelastic motion with fractional diferential operator of damping. Computer Methods Applied Mechanics and Engineer, Vol 19, pp. 5027-5036.

Ji, J. C.; Luo, Q. and Ye, K., 2021, Vibration control-based metamaterials and origami structures: A state-of-the-art review. Mechanical Systems and Signal Processing, Vol. 161, p. 107945.

Jiao, Y., Xu, W., and Song, Y., 2022, Nonlinear response of beams with viscoelastic elements by an iterative linearization method. International Journal of Non-Linear Mechanics, Vol. 146, p. 104132.

Kandasamy, R.., CUI, F., Townsend, N., Foo, C. C., Guo, J., Shenoi, A. and Xiong, Y., 2016 A review of vibration control methods for marine offshore structures. Ocean Engineering, Vol. 127, pp. 279–297.

Kanke, F., Sandmara, L. andPereira, J., T., 2022, “Controle passivo de vibrações em placas via otimização de topologia de camadas restritas (in Portuguese)”, in XI Congresso Nacional de Engenharia Mecânica. CONEN, Teresina, Brasil,

Lanczos, C., 1950. “An iteration method for the solution of the eigenvalue problem of linear differential and integral operators”. *Journal of Research of the National Bureau of Standards*, Vol. 45, p. 255, 1950.

Łasecka-Plura, M., and Lewandowski, R. 2021, The subspace iteration method for nonlinear eigenvalue problems occurring in the dynamics of structures with viscoelastic elements. Computers & Structures, Vol. 254, pp. 106571.

Mainardi, F., 2022. *Fractional calculus and waves in linear viscoelasticity: an introduction to mathematical models.* Imperial College Press, London.

Martin, O., 2016, A modified variational iteration method for the analysis of viscoelastic beams. Applied Mathematical Modelling, Vol. 40, pp. 7988–7995.

Nochebuena-Mora, E., Mendes, N., Lourenço, P. B. and Covas, "J. A, 2021. Vibration control systems: A review of their application to historical unreinforced masonry buildings". *Journal of Building Engineering*, v. 44, p. 103333.

Paige, C. C. and M. A. Saunders, 1975 "Solution of Sparse Indefinite Systems of Linear Equations." *SIAM Journal of Numerical. Analisys*, Vol.12, pp. 617-629.

RAO, S. S., 2011. *Mechanical Vibrations*. Prentice Hall, Upper Saddle River.

Roy, S., Kundu, C. K., 2021, State of the art review of wind induced vibration and its control on transmission towers, Structures, Vol. 29, pp. 254–264.

Saad, Y., 2003. *Iterative Methods for Sparse Linear Systems*. Society for Industrial and Applied Mathematics, Philadelphia.

Silva, F.E.C., 2019. Projeto ótimo de neutralizadores dinâmicos com múltiplos graus de liberdade cosiderando os parâmetros físicos, localização e material viscoelástico (in Portuguese). Master's thesis, Graduate Program in Mechanica engineering, Federal University of Paraná, Curitiba, Brasil.

Tcharkhtchi, A., Nony, F., Khelladi, S., Fitoussi, J., and Farzaneh, S, 2015, Epoxy/amine reactive systems for composites materials and their thermomechanical properties, Advances in Composites Manufacturing and Process Design. Vol 1, pp. 269–296.

Xie, F.; Aly, A. M., 2020, Structural control and vibration issues in wind turbines: A review, Engineering Structures, Vol. 210, p. 110087.

9. RESPONSIBILITY NOTICE

The authors are the only responsible for the printed material included in this paper.